

Stress Distributions in a Semi-infinite Plate Due to a Pin Determined by Interferometric Method

The maximum values of radial pressure and circumferential stress produced around the hole and stress on the free edge in relation to the shape factor are investigated by new method developed by the authors

by M. Nisida and H. Saito

ABSTRACT—The stress distributions in a semi-infinite plate due to a loaded pin of the same material as the plate are systematically investigated by an interferometric method which has been developed by the authors.

For the experiments, a finite plate of diallylphthalate with a circular hole is used. It is supported at one side and loaded in the direction normal to the opposing straight edge by a pin which just fits the hole.

The ratio of the distance e between the hole center and the straight edge to the diameter d of the hole is varied in steps from 4.0 to 1.0.

At each step, the distributions of principal stresses σ_1 and σ_2 along the hole edge, line of symmetry and straight edge, which have not been fully investigated especially when e/d is small, are obtained separately from the isopachic and isochromatic fringes of the interfero-stress patterns. The relations between the maximum values of these stresses and the shape factor e/d are determined.

Introduction

The distributions of stresses or stress concentration at or near a hole in a plate when a load is applied to the pin filling the hole is an important practical engineering problem concerning a rivet or a pin joint. This problem has been treated by Coker,¹ Frocht,² Theocaris³ and other researchers by means of conventional photoelasticity alone or with other auxiliary methods. Coker measured, mechanically, the thickness change of the plate by employing a specially design extensometer, and Theocaris used electrical-potential analogy for tracing stress trajectories.

In a semi-infinite plate with a circular hole which is loaded by a pin, if the plate terminates in a straight edge near the hole, the stresses at both the hole boundary and the straight edge must have high values. Therefore the problem is in finding the maximum values of radial pressure and circumferen-

M. Nisida and H. Saito are Researcher in Chief and Researcher, respectively, Photoelasticity Laboratory, The Institute of Physical and Chemical Research, Komagome, Bunkyo-ku, Tokyo, Japan.

Paper was presented at Second SESA International Congress on Experimental Mechanics held in Washington, D. C., on September 28–October 1, 1965.

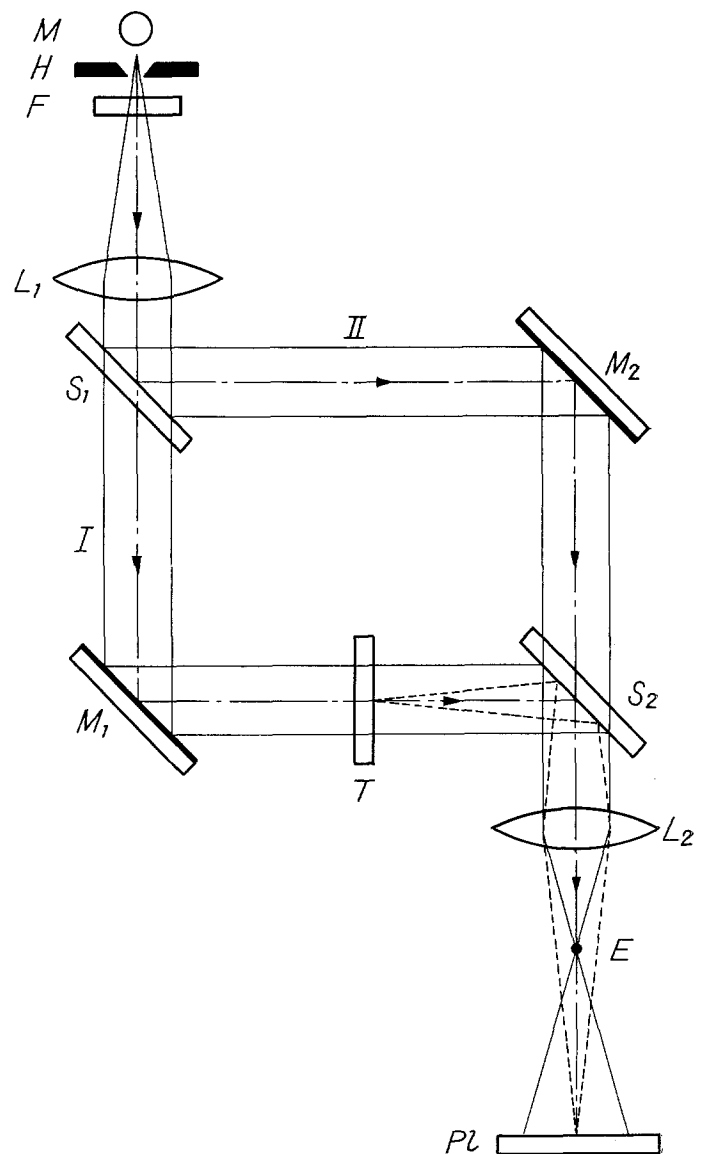


Fig. 1—Schematic diagram illustrating the principle of Mach-Zehnder interferometer. M: mercury lamp, F: filter, Wratten No. 77A; L_1 : collimating lens, L_2 : collecting lens, S_1 , S_2 : beam splitter, M_1 , M_2 : plane mirror, T: test piece

Fig. 2—An example of interfero-stress pattern—contact between a circular disk and a semi-infinite plate

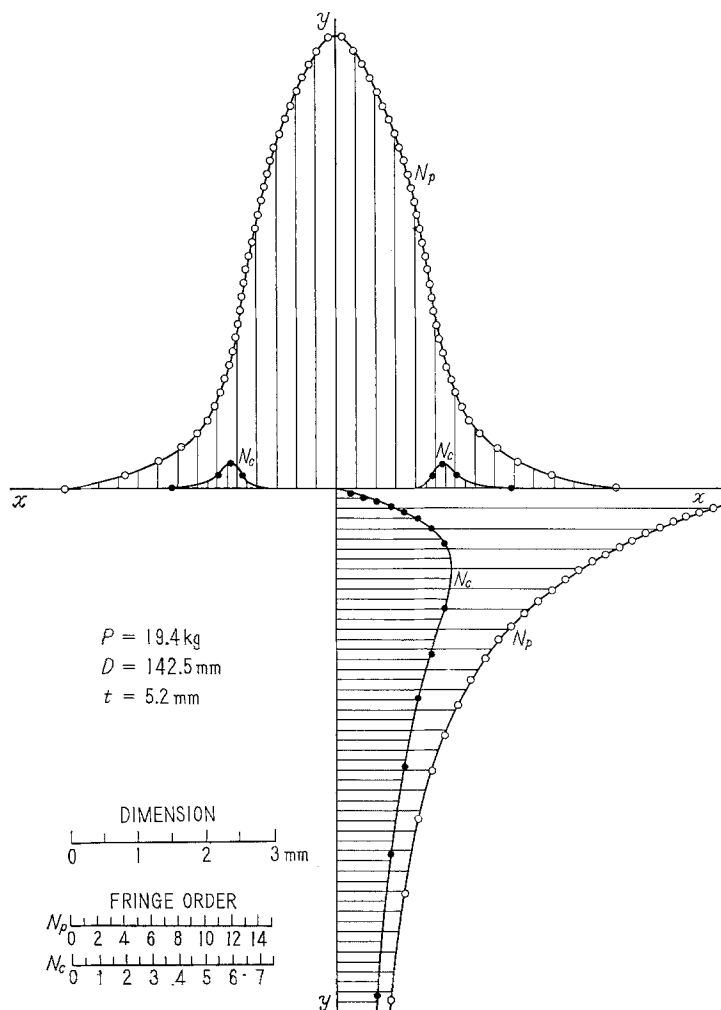
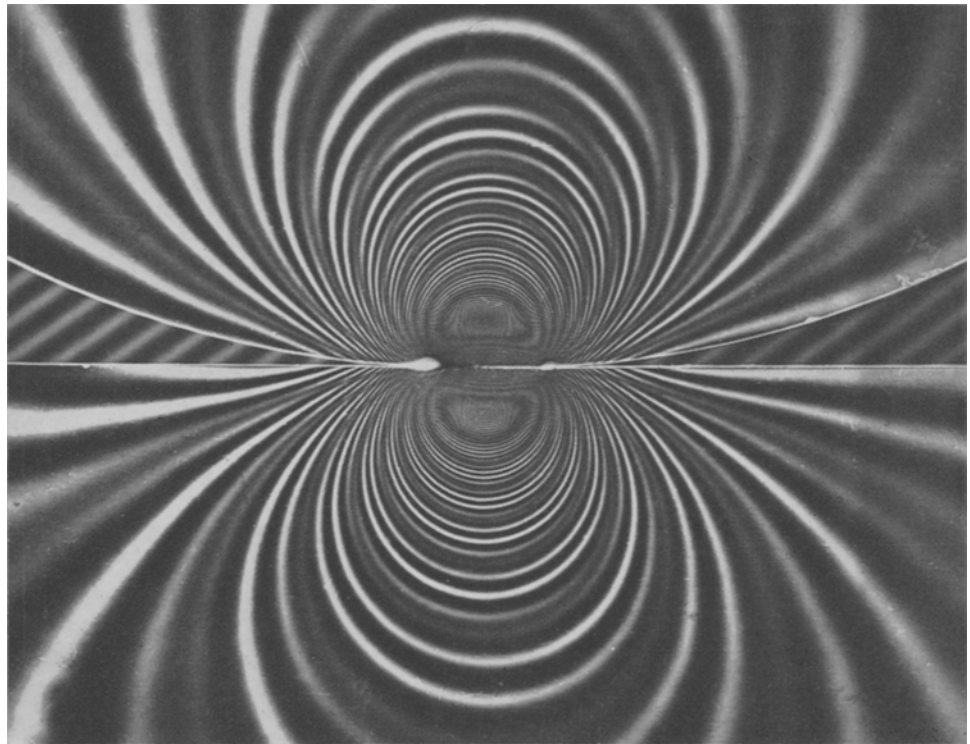


Fig. 3—Distributions of isopachic and isochromatic fringe order, N_p and N_c , obtained from the interfero-stress pattern shown in Fig. 2

tial stress produced around the hole and the stress on the free edge in relation to the shape factor.

In the present study, the stress distributions in the case mentioned above are systematically investigated by an interferometric method developed by the authors. The distributions of principal stresses along chief boundaries are determined separately from the isopachic and isochromatic fringes of the interferometric pattern taken by the method and the relations between the maximum values of these principal stresses and the shape factor e/d are established.

Brief Description of Interferometric Method

In a previous paper by the authors,⁴ it was clarified that when a model of transparent plane parallel plate under two-dimensional stress state is placed in one of the paths of an interferometer, Mach-Zehnder interferometer for example, a pattern which consists of two independent families of fringes—isopachic fringes and isochromatic fringes—is obtained (see Fig. 1).

If t denotes the thickness of the model plate and λ the wavelength of the light used, the light intensity J' in the field is expressed as

$$J' = \frac{1}{2} + \frac{1}{2} \cos \left[\frac{2\pi}{\lambda} \frac{A' + B'}{2} (\sigma_1 + \sigma_2)t \right] \times \cos \left[\frac{2\pi}{\lambda} \frac{A' - B'}{2} (\sigma_1 - \sigma_2)t \right] \quad (1)$$

where A' and B' are the material constants of the model relating to the change of refractive indices of the material and the change of thickness of the model plate due to stress and strain. The values of

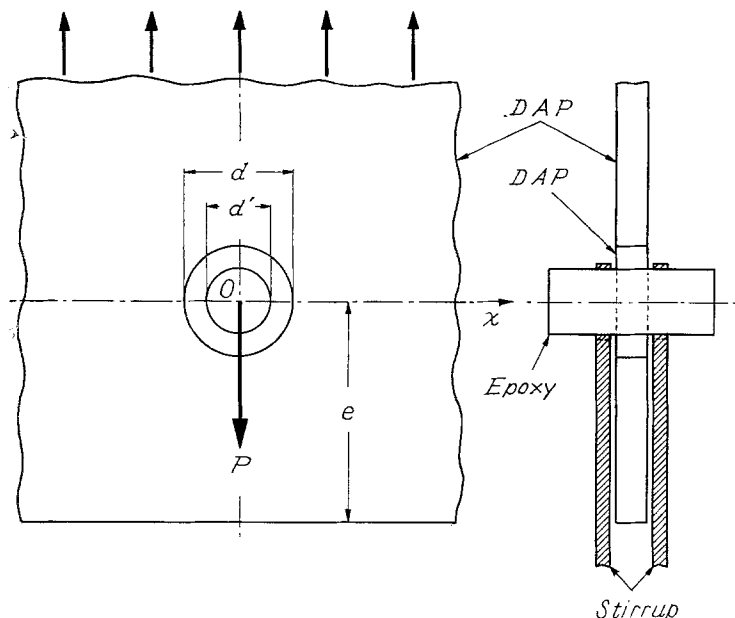


Fig. 4—Illustration of model and loading apparatus

these constants for diallylphthalate used in the present investigation were found to be as follows:

$$A' = -103, B' = -142, A' + B' = -242,$$

$$A' - B' = C = 42 (\times 10^{-5} \text{ mm}^2/\text{kg})$$

It is seen from eq (1) that the distribution of light intensity of the interference pattern depends not only on the value of $\sigma_1 + \sigma_2$ but also on the value of $\sigma_1 - \sigma_2$ at every point.

The intensity J' at a point where $(2\pi/\lambda)(A' - B')(\sigma_1 - \sigma_2)t = 2m\pi$ (m : integer, $A' - B' = C$: Brewster's constant), i.e., at a point on a line that corresponds to a black isochromatic line in an ordinary dark-field photoelastic pattern, is expressed as

$$J' = \frac{1}{2} + \frac{1}{2} \cos \left[\frac{2\pi}{\lambda} \frac{A' + B'}{2} (\sigma_1 + \sigma_2)t \right] \quad (2)$$

whereas the intensity at a point where $(2\pi/\lambda)(A' - B')(\sigma_1 - \sigma_2)t = (2m + 1)\pi$, i.e., at a point on a line corresponding to a black isochromatic line in a bright-field photoelastic pattern becomes

$$J' = \frac{1}{2} \quad (3)$$

This means that the halftone or the little-indistinct lines that represent the isochromatic lines along which $\sigma_1 - \sigma_2 = \text{constant}$ as in photoelasticity, appear over the pattern running through the family of isopachic fringes which are contour lines of $\sigma_1 + \sigma_2$, and these bright and dark stripes of the isopachic pattern are reversed in intensity across every isochromatic line. Therefore the pattern obtained by this method permits direct and simple evaluation of interior principal stresses separately.

As an example, an interferometric pattern obtained with contact between a circular disk and the straight edge of a semi-infinite plate is shown in Fig. 2. From the pattern, the distributions of isopachic fringe order N_p and isochromatic fringe order N_c

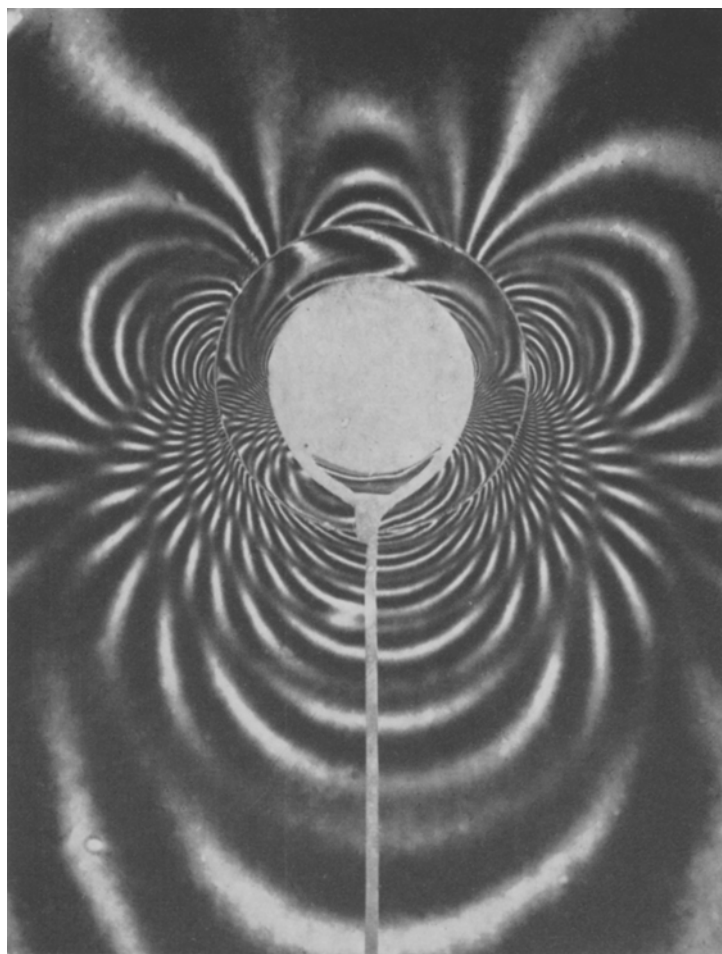


Fig. 5—Interfero-stress pattern of an infinite plate loaded by a circular pin. ($e/d = 4.0$)

along the lines of concern are plotted as shown in Fig. 3.

Test Pieces and Loading

Plane-parallel plates with no appreciable inhomogeneity of refractive index used in this method can be prepared, although not very easily, by casting an appropriate material such as diallylphthalate (DAP) between two optically flat glass plates.

A rectangular plate of DAP, $200 \times 200 \times 5.34$ mm³ in size, Young's modulus $E = 224$ kg/mm² and Poisson's ratio $\nu = 0.41$, has at its center a circular hole of 20 mm in diameter into which a close-fitting annular disk of the same material and thickness as the plate was inserted with lubricant.

An epoxy pin, 12 mm in diameter, was passed through the center of the inserted disk and a load P was applied to the pin by a pair of stirrups in the direction normal to the straight edge of the plate, the opposing side being fixed by a row of small pins (see Fig. 4).

Figure 6 is an ordinary photoelastic pattern obtained with the used model for $e/d = 4.0$. It corresponds to the stress distribution of interferometric pattern shown in Fig. 5. This figure is men-

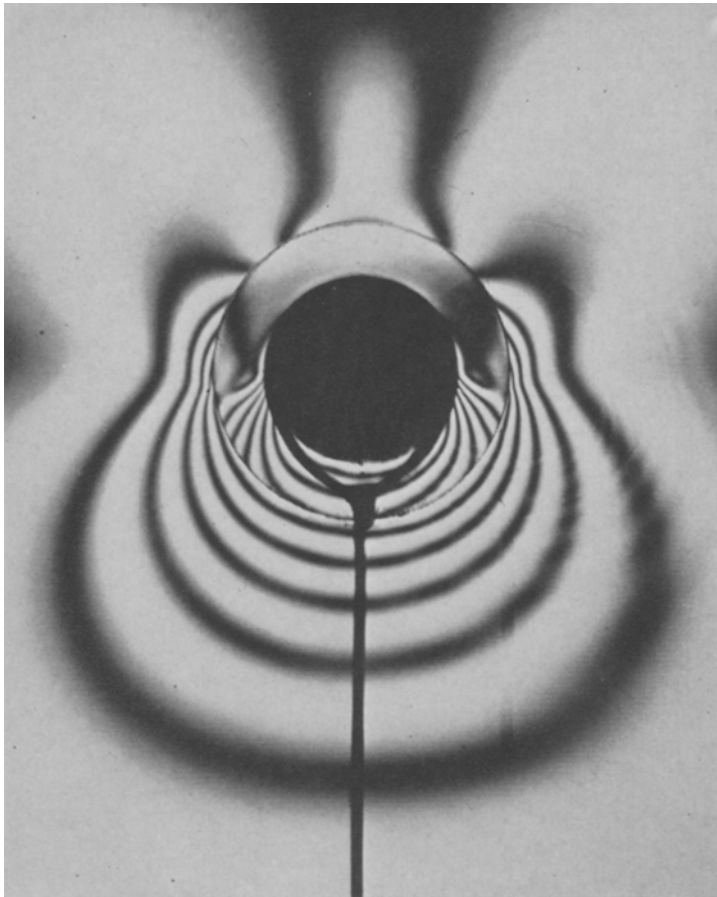


Fig. 6—Isochromatic fringe pattern obtained by ordinary photoelasticity which corresponds to the case shown in Fig. 5 for comparison

tioned here to show that the model had a sufficiently large area to be taken for a plate of semi-infinite expansion, for we see little influence of the nearness of the boundaries on the stress state near the hole. It is also seen from the figure that the contact between the hole edge and the boundary of the pin is satisfactorily smooth and regular since no ruggedness or disturbance of the fringes is found near the hole edge.

It is obvious that the distribution of stresses at and near the edge of the hole will be greatly influenced by the condition of contact between the pin and the hole boundary. Even the slightest unevenness of the contact surface produces rather remarkable ruggedness or disturbance of the isopachic and isochromatic fringes which lead to irregularity of the results. Moreover, it is easily understood that the degree of fitting of the pin into the hole affects not a little the distributions of stresses. If there exists any appreciable clearance, the contact surface would be restricted to a small area and, when loaded, the hole would be less prevented by the disk from deforming.

In our case, the pin was machined precisely on a lathe to fit the hole so smoothly and uniformly that at no load there was no appreciable initial clearance nor pressure across the boundary.

Furthermore, in applying the results obtained on plastic models to metal structure, the differences in elastic constants and, also, the difference in frictional states of the contact surfaces should be taken into consideration; nevertheless, practically these differences do not seem so large as to impair



Fig. 7—Interfero-stress pattern of a semi-infinite plate loaded by a circular pin. ($e/d = 1.0$)

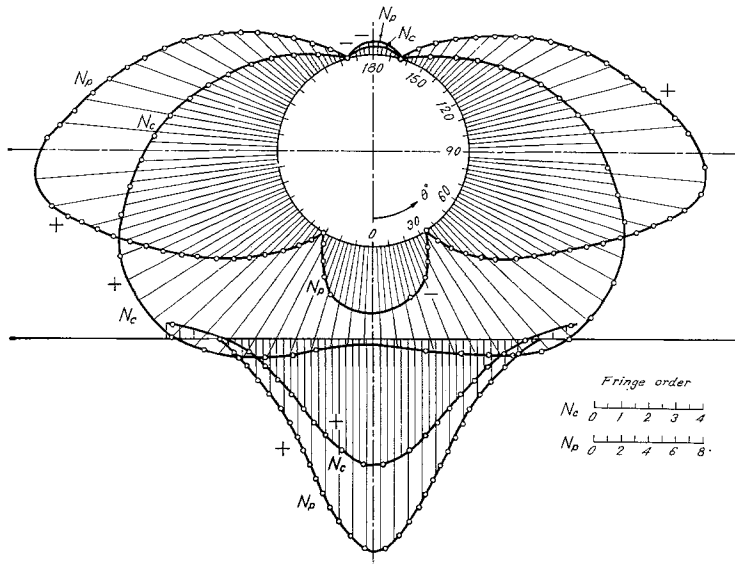


Fig. 8—Example of diagram showing the distributions of isopachic and isochromatic fringe order, N_p and N_c , along circular and straight edge. ($e/d = 1.0$)

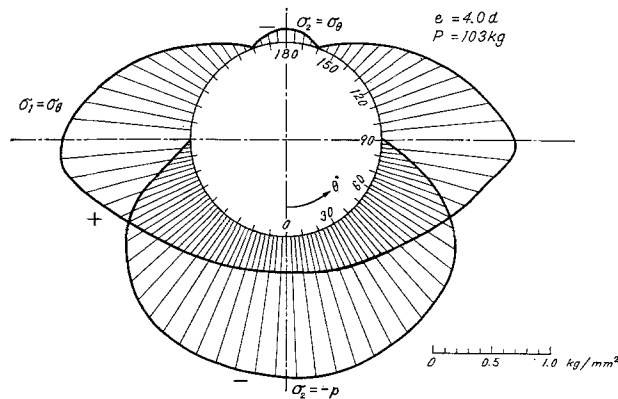


Fig. 9—Principal stress distributions along circular edge. ($e/d = 4.0$)

the generality of the experimental results.

When the interferometric pattern was photographed for one shape factor e/d , the plate was cut to give the next shape factor. The cutting was done with care not to affect the state of contact between the hole and the pin. In this way, one plate with pin served us for a series of experiments with four shape factors

$$e/d = 4.0, 2.5, 1.5, 1.0$$

Results

Some typical interferometric patterns obtained by the previously mentioned method are shown in Fig. 5 and Fig. 7 of which is $e/d = 4.0$ ($P = 103 \text{ kg}$) and 1.0 ($P = 63 \text{ kg}$), respectively.

In Fig. 8, the distributions of isopachic and isochromatic fringe orders (N_p and N_c) for the case $e/d = 1.0$ obtained from the interferometric pattern in Fig. 7 are shown.

The distributions of pressure p and circum-

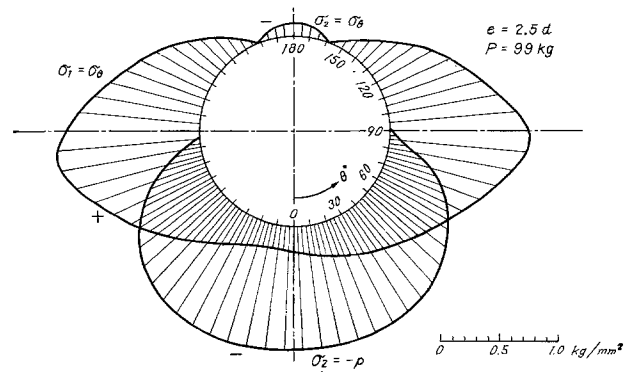


Fig. 10—Principal stress distributions along circular edge. ($e/d = 2.5$)

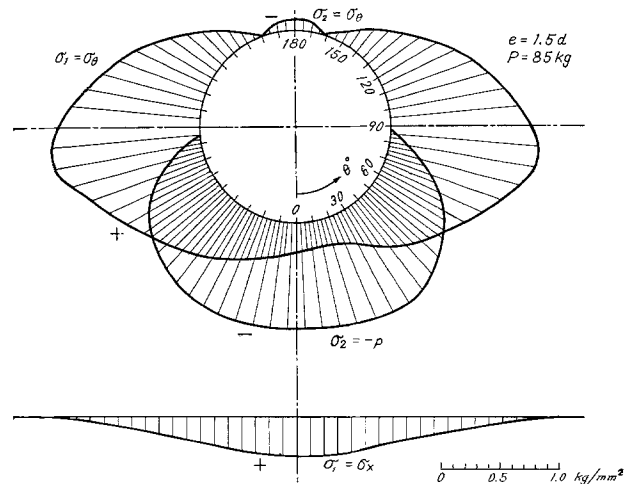


Fig. 11—Principal stress distributions along circular and straight edge. ($e/d = 1.5$)

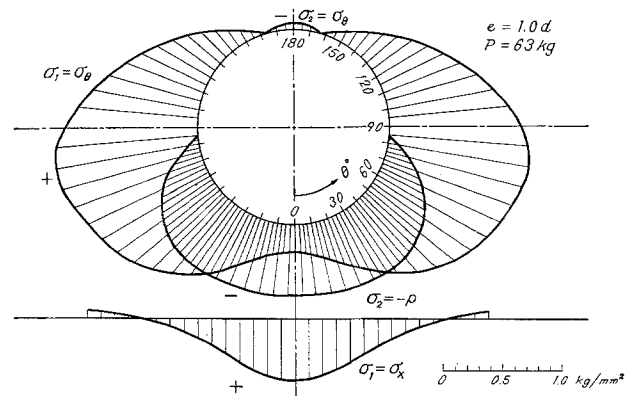


Fig. 12—Principal stress distributions along circular and straight edge. ($e/d = 1.0$)

ferential stress σ_θ along the hole edge and boundary stress σ_x on the straight edge under load for various shape factors are plotted in Fig. 9 ($e/d = 4.0$, $P = 103 \text{ kg}$), Fig. 10 ($e/d = 2.5$, $P = 99 \text{ kg}$), Fig. 11 ($e/d = 1.5$, $P = 85 \text{ kg}$) and Fig. 12 ($e/d = 1.0$, $P = 63 \text{ kg}$). Strictly speaking, principal stresses σ_1 and σ_2 do not coincide with σ_θ and p , respectively, because of the frictional force that acts on the boundary between the hole and the pin by the relative deformation and displacement when loaded,

Fig. 13—Distributions of pressure p and tangential stress σ_θ along circular edge for various factors, e/d ($P = 100$ Kg, $t = 5.34$ mm)

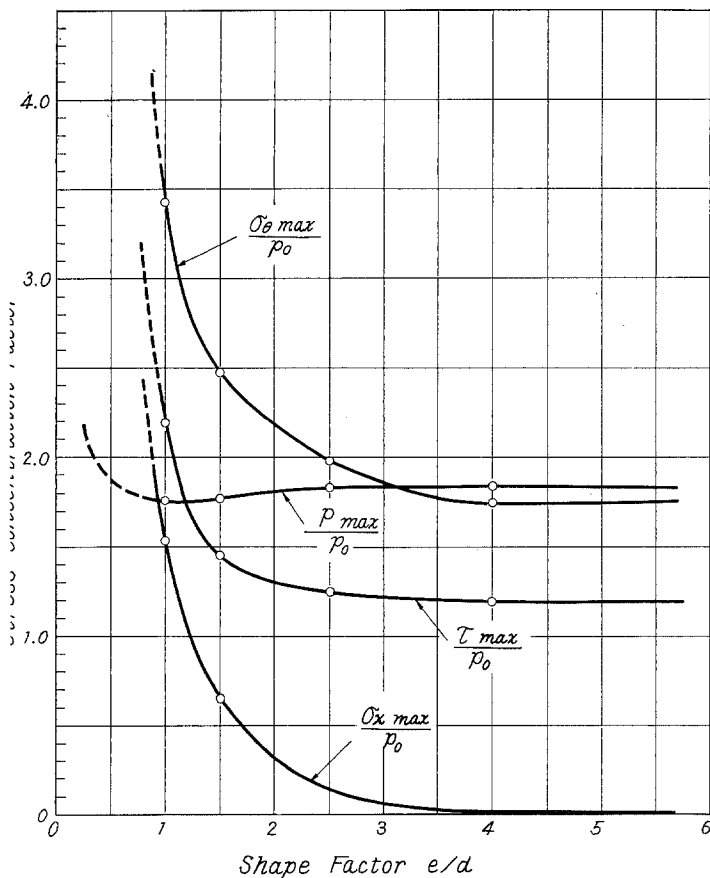
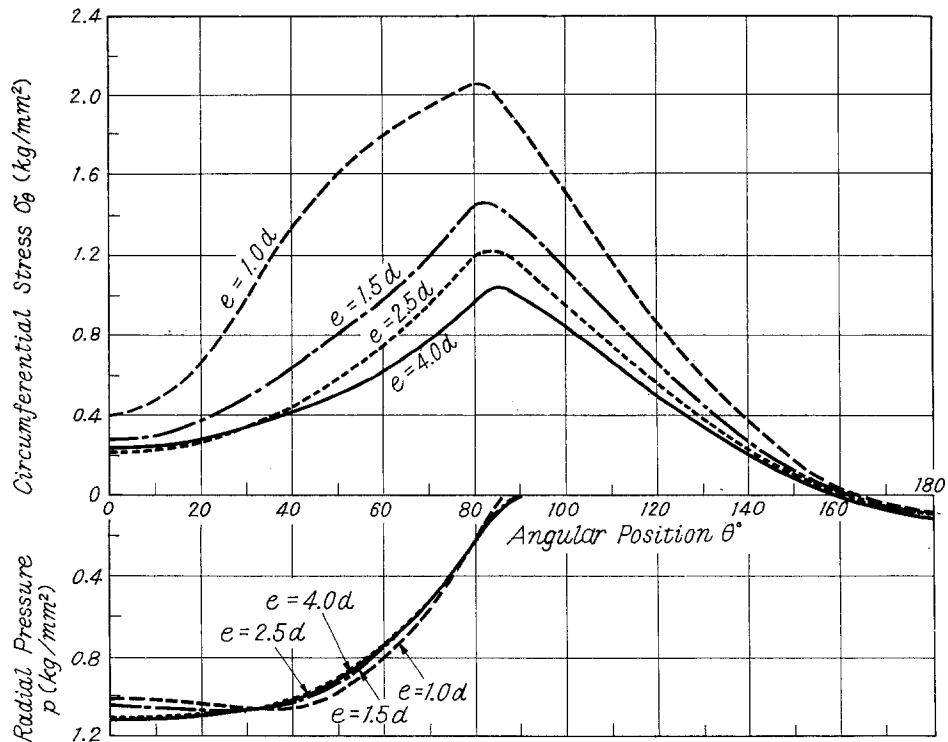


Fig. 14—Relations between stress-concentration factors and shape factor

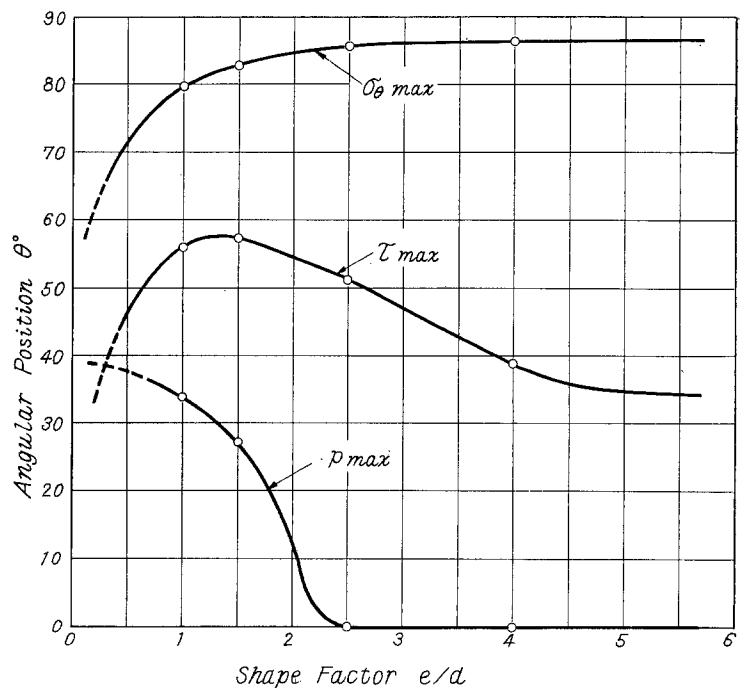


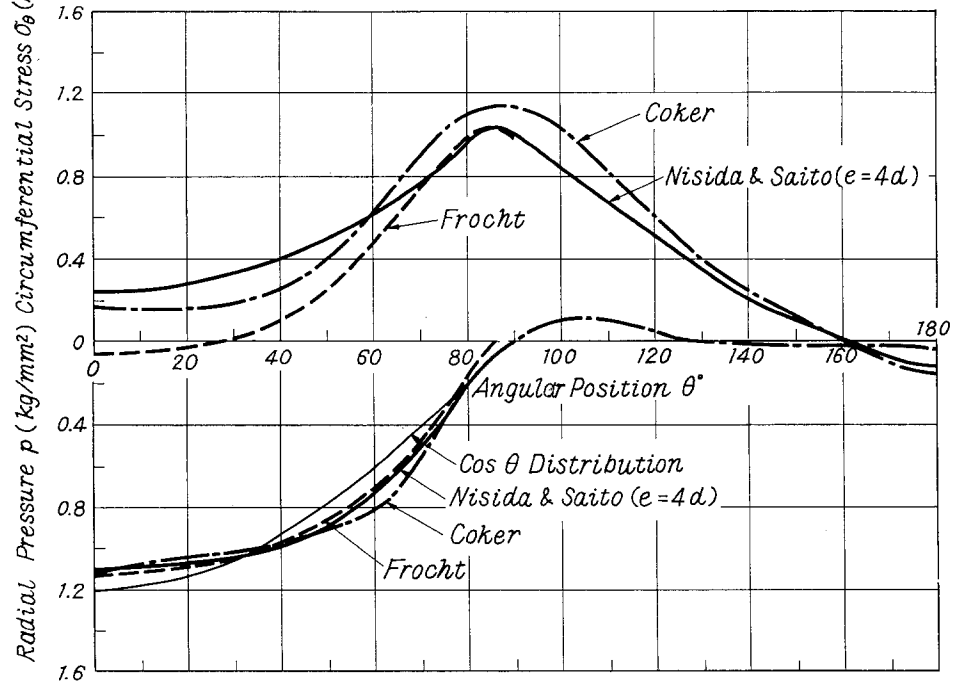
Fig. 15—Relations between angular position of maximum stresses and shape factor

but this discrepancy has been proved to be very small and practically negligible.

Figure 13 shows, as a summary of these results, the distribution of p and σ_θ on the hole edge for a standardized load $P = 100$ kg ($t = 5.34$ mm) with e/d as a parameters, the abscissa θ being the angle measured from the direction of the applied load.

An interesting feature in this two-dimensional

Fig. 16—Comparison of stress distributions obtained by Coker, Frocht and the authors ($P = 100$ Kg, $t = 5.34$ mm)



elastic problem is how the maximum of σ_θ that occurs at about $\theta = 85$ deg varies with the shape factor e/d . This is shown in Fig. 14 together with the variation of p_{\max} and τ_{\max} on the hole edge and $\sigma_{x\max}$ on the straight edge. In the figure, the ordinate represents the ratio of the above four quantities to a standard pressure $p_0 = 2P/\pi td$.

As is easily expected, $\sigma_{\theta\max}$, $\sigma_{x\max}$ and τ_{\max} increase with the decrease of e/d , all tending to infinity when e/d approaches zero, while, for values of e/d larger than about 4.0, they are constant. This means that 4.0 is the necessary and sufficient value of e/d from the viewpoint of strength of structure.

Another noteworthy feature of the results is that, when e/d is small, radial pressure p shows its maximum value at some distance from center line, whereas when e/d is large, the maximum pressure occurs on the point of symmetry. This means that, when e/d is small, the center part of the ligament is no longer rigid enough to support the load, which is now borne mainly by its two broader sides.

Figure 15 shows the relation of e/d to locations of p_{\max} , $\sigma_{\theta\max}$ and τ_{\max} .

Discussion

In Fig. 11, we see that when $e/d = 4.0$, the distribution of σ_θ is a little anomalous in comparison with the cases of other values of e/d . This is likely due to a slight difference of the state of contact caused by the break-in of the pin during repeated loading.

It is also interesting to compare the results of the authors' work with those of Coker and Frocht for large e/d .

As shown in Fig. 16, Coker and Frocht give undeniably different distributions of σ_θ and p . The cause of this difference seems to rest on the fact that, in Frocht's case, there was a slight clearance of about 0.01 mm between hole and pin, and in Coker's case, mechanical measurements of the strain were not made just on the boundary but at 0.25 mm outside of it.

As for the distribution of radial pressure p on the circular boundary, the usually conceived $\cos \theta$ distribution was found not to agree with the experimental results even for large values of e/d .

Summary

The stress distributions in a pin-loaded semi-infinite plate were investigated systematically for various values of shape factor e/d by an interferometric method.

The relations of shape factor to maximum values of circumferential stress σ_θ , radial pressure p along the hole edge, and stress σ_x on the straight edge have been established.

The results were discussed from the viewpoint of the condition of contact between the hole and the pin.

References

1. Coker, E. G., and Filon, L. N. G., *T. on Photoelasticity*, Cambridge Univ. Press, 524-532 (1931).
2. Frocht, M. M., *Photoelasticity*, John Wiley, 1, 281-286 and 309-322 (1949).
3. Theocaris, P. S., "On an Electrical Analogy Method for the Separation of Principal Stresses along Stress Trajectories," *Proc. SESA*, XIV (2), 11-20 (1957).
4. Nisida, M., and Saito, H., "A New Interferometric Method of Two-dimensional Stress Analysis," *EXPERIMENTAL MECHANICS*, 4 (12), 366-376 (1964).